

MECHANOCHEMICAL SYNTHESIS OF BISMUTH FERRITE**Z. Marinković Stanojević^{a,*}, L. Mančić^b, T. Srećković^a, B. Stojanović^a**^a Institute for Multidisciplinary Research, University of Belgrade, Serbia^b Institute of Technical Sciences SASA, Belgrade, Serbia

(Received 30 April 2012; accepted 12 October 2012)

Abstract

A powder mixture of Bi_2O_3 and Fe_2O_3 was mechanically treated in a planetary ball mill in an air from 30 to 720 minutes. It was shown that the mechanochemical formation of BiFeO_3 (BFO) phase was initiated after 60 min and its amount increased gradually with increasing milling time. A detailed XRPD structural analysis is realized by Rietveld's structure refinement method. The resulting lattice parameters, relative phase abundances, crystallite sizes and crystal lattice microstrains were determined as a function of milling time. Microstructural analysis showed a little difference in morphology of obtained powders. The primary particles, irregular in shape and smaller than 400 nm are observed clearly, although they have assembled together to form agglomerates with varying size and morphology. Dense BFO ceramics were prepared by conventional solid-state reaction at the temperature of 810°C for 1h followed immediately by quenching process.

Keywords: Milling, Structure, X-ray method, BiFeO_3 .**1. Introduction**

Materials that combine magnetic and ferroelectric properties have generated increasing interest over the last few years, due to the potential application for new electronic devices. A great attention has attracted bismuth ferrite, which shows ferroelectric and ferromagnetic properties at room temperature [1, 2]. Bismuth ferrite (BiFeO_3) has perovskite structure and this group usually is fabricated by convention solid state reaction at high temperatures. However, preparation of phase-pure bismuth ferrite is reported to be difficult. During synthesis, the kinetics of formation always leads to a mixture of BiFeO_3 as a major phase along with the impurity phases such as $\text{Bi}_2\text{Fe}_4\text{O}_9$ and $\text{Bi}_{25}\text{FeO}_{39}$. Researchers have suggested different reasons for the appearance of the secondary phases. They describe bismuth ferrite as being metastable, off-stoichiometric, having a low peritectic decomposition temperature etc [3-6].

In recent years, many techniques have been employed to produce single-phase magnetoelectric oxide materials [7-13]. Among them, the high-energy ball milling techniques has emerged as an attractive alternative [14-16]. High-energy ball milled products usually show high defect density, large surface area and enhanced diffusion rates [16]. Mechanochemical synthesis commonly refers to solid-state reactions

initiated by intensive milling in high-energy ball mills. Nucleation process is initiated at room temperature, exhibiting distribution that is more homogeneous. Generation of smaller particles with larger specific surface area, compared with those prepared by conventional solid state method, is commonly achieved [15].

In order to optimise the synthesis and sintering process to produce more stable product we have studied the formation of BiFeO_3 from the starting oxides Bi_2O_3 and Fe_2O_3 through mechanochemical reaction to the final ceramic product.

2. Experimental procedure

Mixtures of starting Bi_2O_3 (Alfa Aesar, p.a. 99%) and Fe_2O_3 (Superlab, p.a. 99%) powders in equimolar quantities were used in experimental procedures. Mechanical activation was performed by dry grinding (air atmosphere) in a continual regime in a planetary ball mill (Fritsch Pulverisette 5) during 30, 60, 120, 240, 360 and 720 min. Samples were denoted as BFO30 to BFO720 according to time of activation. The rotational speed of the disk was 325 rpm and of the vials about 400 rpm. The distance between the rotational axes was 125 mm. Stainless steel grinding balls (32 balls of approx. 12 mm in diameter, $\rho = 7.874 \text{ g/cm}^3$) and two cylindrical bowls (100 mm in

* Corresponding author: mzorica@imsi.bg.ac.rs

diameter, 80 mm in height) were used. Based on those values the ball-impact energy ($\Delta E_b^* = 81$ mJ/hit), the weight-normalized cumulative energy introduced to the system during milling until the BFO phase was formed ($E_{cum} = 101$ kJ/g) are calculated according to the assumption proposed and elaborated by Burgio et al. [17].

The BFO ceramics were prepared from mechanochemically obtained powders by conventional solid state reaction followed immediately by quenching process. The ground powder mixtures were uniaxially pressed in steel dies into pellets (10 mm in diameter) at 125 MPa. The discs were sintered at 810°C for 1h in air, and then quenched to room temperature. The relative density value of ~ 90% was obtained for sample BFO240, while samples BFO360 and BFO720 possess smaller relative density of about 85%.

The phase composition and structure of the obtained powders were characterized by X-ray powder diffraction (XRPD). X-ray diffraction data of all mechanically treated samples were recorded using a Bruker D-5000 diffractometer equipped with a graphite monochromator using CuK_{α} radiation operating at 30mA and 40kV. XRD patterns were collected in the range of 20-70° (2 θ) with a step size of 0.02° and improved counting time of 16s. Specific surface area, S_{BET} , of starting oxides and mechanically activated mixtures were determined by isothermal nitrogen physisorption (BET method, Micromeritics Flow Sorb II 2300). The equivalent BET particle diameter, d_{BET} , was calculated by the formula $d_{BET} = 6/\rho \cdot S_{BET}$. The particle size distribution (PSD) and mean particle size of selected samples were measured in the liquid mode using a laser particle size analyzer (Microtrac S3500). Particle morphology was characterized by scanning electron microscopy (SEM TESCAN Vega TS 5130MM).

3. Results and Discussion

X-ray diffractograms of powder mixtures milled for various times are presented at Fig.1. It is evident from this figure that in the course of ball milling of mixtures, the $BiFeO_3$ phase has been formed and its amount increased very quickly with increasing milling time. Broadening of diffraction peaks indicated that a significant refinement in crystallite size in initial oxides have been induced prior of $BiFeO_3$ nucleation. Upon 60 min milling, new broad peaks of perovskite bismuth ferrite phase are formed indicating the beginning of mechanochemical reaction in the system. This is significantly shorter time in comparison to conditions given by other authors that reported formation of $BiFeO_3$ nanopowder after 70 hours of milling [14]. One of the possible explanations of such a great mismatching in

milling time could be a different mechanics of the mills used for synthesis, resulting in a different amount of energy that could be transferred to powder during milling. In our case, $BiFeO_3$ was detected at cumulative kinetic energies of about 101 kJ/g. In literature was found that a minimum cumulative kinetic energy ranging from 10 to 150 kJ/g is necessary to trigger the mechanochemical formation of other perovskite structures [15].

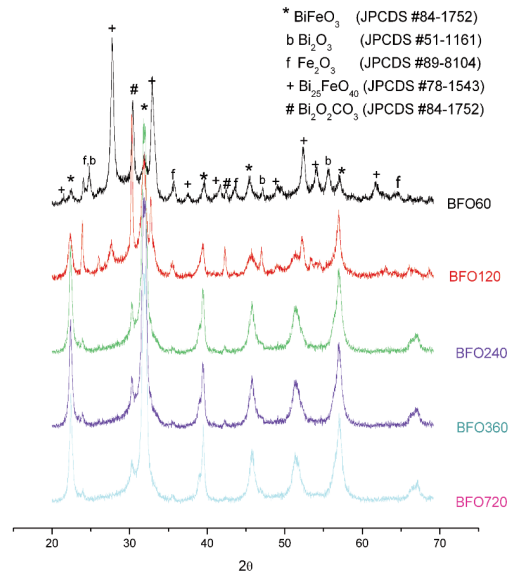


Figure 1. XRPD patterns of BFO powders after different stages of the mechanochemical synthesis.

After 240 min of synthesis, majority of the reflection peaks can be indexed as $BiFeO_3$ rhombohedrally distorted perovskite belonging to the space group $R3c$. Intensity profile of the reflection peaks are close to those reported in JCPDS (# 86-1518). The appearances of these diffraction peaks prove that $BiFeO_3$ can grow at room temperature without any additional crystallization step. All peaks are very broad owing to the fact that the primary crystallite size in the synthesized $BiFeO_3$ powders is rather small. In order to follow the evolution of the $BiFeO_3$ mechanochemical formation, the structural refinements of all obtained powders were done by Rietveld-based software Topas-Academic [20]. For example, Fig.2 shows the quality of profile fitting in the sample BFO120. The lattice parameters, as well as the crystallite size and the microstrain have been estimated and they are given in Table 1. It is evident from Table 1 that obtained bismuth ferrite particles were composed of primary nanocrystallites smaller than 22 nm. The structural changes expressed through the crystallite size imply a little increase of crystallinity with increasing milling time up to 240 minutes and after that this value remains almost

unchanged with prolongation of milling. On the other hand, after 60 min of the mechanochemical synthesis the value of microstrain of the crystal lattice achieving maximum and then started to decrease. This finding may indicate that in the beginning of the milling process most of the crystal lattice imperfections are generated, while further milling leads to the structural relaxation. The lattice parameters of the mechanochemically synthesized BiFeO_3 phases are significantly high in comparison to JCPDS 86-1518 reported values ($a=5.5775 \text{ \AA}$, $c=13.8616 \text{ \AA}$), especially for the sample BFO60. For the lattice parameters a similar trend as that of microstrain are observed. They are decrease non-linearly and continuously, moving up to the reported values with increasing time of synthesis (see Table 1).

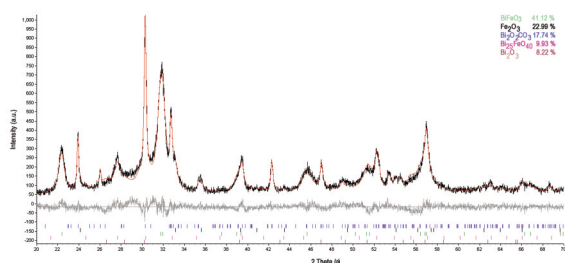


Figure 2. Final Rietveld plot obtained by refinement of the X-ray pattern of the BFO120 sample ($R_{wp} = 10.69\%$, $R_{Bragg} = 1.94\%$).

Table 1. Crystallographic data of mechanothesized BiFeO_3 estimated from the Rietveld analysis [15].

Sample	Unit-cell parameter			
	a , [Å]	c , [Å]	Crystallite size [nm]	Microstrain [%]
BFO60	5.598(3)	13.98(1)	18(4)	1.26(3)
BFO120	5.595(1)	13.854(8)	16.6(6)	0.95(1)
BFO240	5.5857(4)	13.867(2)	21.8(4)	0.61(5)
BFO360	5.5808(7)	13.854(2)	21.2(4)	0.57(5)
BFO720	5.5822(7)	13.862(3)	21.3(4)	0.45(5)

Fig. 3 shows the results of quantitative XRPD analysis, made as a part of structural refinement [20]. The results illustrate the evolution of second phases with increasing milling time. The presence of these impurities was not surprising and its main peaks are indicated in the Fig.1. It can be seen that at a shorter milling time, in the samples BFO60 and BFO120, the second phase is mainly $\text{Bi}_{25}\text{FeO}_{40}$ which than subsequently transforms to BiFeO_3 with prolonged milling. The formation of BiFeO_3 phase is noticed in 60 min milled sample and its wt% increasing continuously from value of 9%, reaching a maximum

value of about 84% in sample milled 720 min. The samples BFO240, BFO360 and BFO720 mainly consisted of BiFeO_3 phase with minor contamination by bismuth oxycarbonate ($\text{Bi}_2\text{O}_2\text{CO}_3$) and traces of unreacted Fe_2O_3 and hexagonal Bi_2O_3 which is the high pressure polymorphs of Bi_2O_3 [21]. $\text{Bi}_2\text{O}_2\text{CO}_3$ is an orthorhombic phase, with a layered structure, easily stabilized at high pressure [21, 22]. It originates from the contamination of the surface of the starting oxides (in particular of bismuth oxide) by atmospheric CO_2 due to reaction performed in a confined and theoretically closed volume [21, 23]. The decomposition of carbonate to oxide is facilitated after the mechanochemical reaction during the thermal treatment of obtained powders.

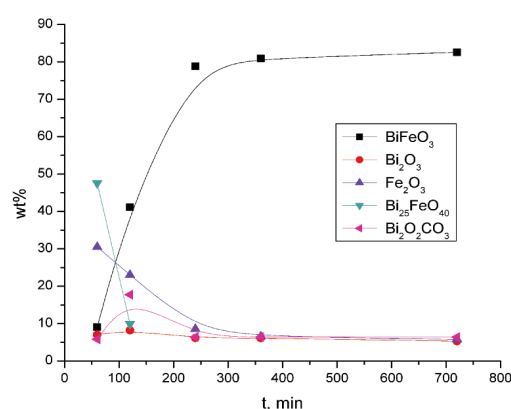


Figure 3. Quantified phase percentages obtained from full pattern Rietveld refinement of X-ray data sets during the mechanochemical synthesis of BiFeO_3 .

Values of the specific surface area of the investigated powders are given in Table 2. Specific surface area doesn't follow a clear trend with time of activation due to the secondary processes like agglomeration. The specific surface area changes during milling process and depend on whether the

Table 2. Results of the specific surface area measurements and particle size distribution.

Sample	Sp [m ² /g]	D_{BET} [μm]	D_{v10} [μm]	D_{v50} [μm]	D_{v90} [μm]	<1μm [%]
Bi_2O_3	0.28	2.425	-	-	-	-
Fe_2O_3	5.99	0.191	-	-	-	-
BFO30	1.82	0.436	-	-	-	-
BFO60	1.5	0.539	-	-	-	-
BFO120	1.63	0.487	0.193	0.352	2.27	80.66
BFO240	2.93	0.271	0.163	0.357	1.455	86.37
BFO360	2.69	0.295	0.169	0.366	1.657	85.35
BFO720	3.04	0.261	-	-	-	-

breaking processes of the starting material or the agglomeration dominates. The agglomeration of particles occurred in two stages, after 30 and 240 min.

Particle size measurements, performed for selected samples BFO120, BFO240 and BFO360, show influence of the milling time on the particle size distribution (see Table 2). The particle size distribution follows quite well a log-normal distribution with the prevalence of the small size particle fractions in all monitored samples. The median particle size, $D_{v,50}$, estimated to be about 360 nm (Table 2). The calculated equivalent BET diameter, D_{BET} , for samples BFO240 and BFO360 are smaller than the median particle size values for about 25%. In the case of BFO120 sample, D_{BET} is higher than the median particle size for 35%. The observed discrepancy is presumably the consequence of the irregular shape of particles and the wide particle size distribution due to existence of the large agglomerates in powders, rather than the particle porosity, as observed in accordance to the SEM examination (Fig. 4). Results obtained from the particle size distribution are in good agreement with values of the specific surface area.

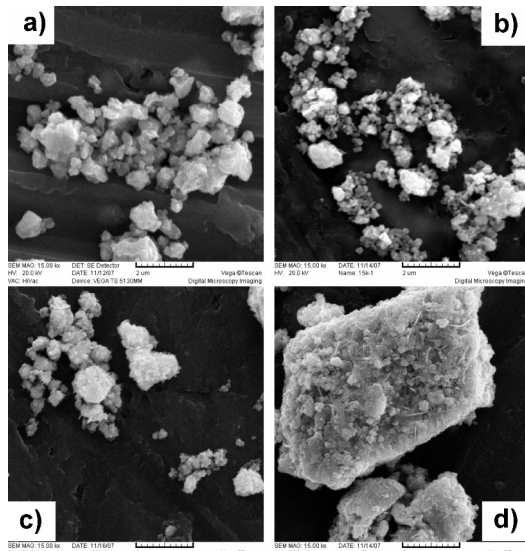


Figure 4. SEM images of powders a) BFO120, b) BFO240, c) BFO360 and d) BFO360 (an agglomerate structure).

Microstructural analysis showed a little difference in morphology of obtained powders (Fig. 4a, 4b and 4c). The primary particles, irregular in shape and smaller than 400 nm, are observed clearly, although they have assembled together to form agglomerates with varying size and morphology. Very large forms, from 2 to 5 μm , are noticeable occasionally in all investigated samples. For example, one of agglomerated structure of the powder BFO360 is

shown in Fig.4d. Visible surface of agglomerates revealed rough and composite structure, which representing set of the smaller particles. A typical morphology of agglomerates implies higher degree of the primary particle bonding, indicating that powder obtained through mechanochemical process is very reactive. However, production of the finer powders is evident with prolonged milling. Agglomeration is expectable when one takes into consideration that the energy input during milling is sufficient to break the coarse particles of the starting powders and to renew the particle contact area resulting in a further particles interaction. Results of SEM analysis are in accordance of the conclusions based on BET calculations.

The XRD spectrum of the well-crystallized BFO240 ceramic after sintering is shown in Fig.5. The reflection peaks are clearly distinguishable, and can be perfectly indexed as a rhombohedrally $R3c$ perovskite BFO structure with the unit-cell parameters, $a=5.578 \text{ \AA}$ and $c=13.868 \text{ \AA}$. However, very small intensity diffraction peak at $2\theta \sim 28^\circ$ was identified as $\text{Bi}_2\text{Fe}_9\text{O}_4$ (JCPDS 74-1098) secondary phase. It is believed that slight contamination of the Fe ions originating from the milling media during milling process, affects the formation of a small amount of Fe-rich $\text{Bi}_2\text{Fe}_4\text{O}_9$ secondary phase. Fig. 6 shows an SEM image taken from polished surface of the BFO240 sample sintered at 810°C for 1h and quenched to room temperature. The measured grain size varied between 0.3 and 1.2 μm in length across the sample surface. The SEM images prove a low level of porosity of the obtained BFO ceramics. Nevertheless, it is necessary to further optimize the milling parameters and sintering conditions in order to improve ceramic properties. This will be the aim of our future investigation.

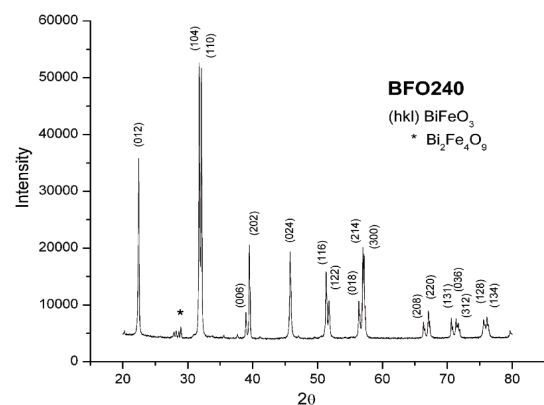


Figure 5. XRD pattern taken of the BFO240 sintered at 810°C , 1h.

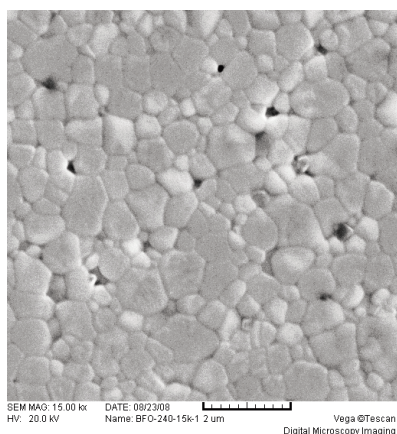


Figure 6. SEM micrograph taken of BFO240 sintered at 810°C for 1h.

4. Conclusions

It was demonstrated that bismuth ferrite can be successfully synthesized by mechanochemical method directly from starting oxides Bi_2O_3 and Fe_2O_3 at room temperature. The formation of BiFeO_3 phase was initiated after 60 min at critical cumulative kinetic energy smaller than 101 kJ/g. It is significantly shorter time in comparison to conditions given by some other investigators. After 240 min of mechanochemical synthesis we obtained nanocrystalline powders which mainly consisted of BiFeO_3 with small contamination by $\text{Bi}_2\text{O}_2\text{CO}_3$, Fe_2O_3 and Bi_2O_3 . It was observed that great changes in phase composition and microstructural parameters could happen up to 240 min of the high-energy milling. The structural changes expressed through crystallite size imply a little increase of crystallinity with the milling time. The particle size distribution follows quite well a log-normal distribution with the prevalence of the small-sized particle fraction. The primary particles, irregular in shape and smaller than 400 nm, are observed clearly, although they have assembled together to form agglomerates with varying size and morphology. The agglomeration of particles occurred in two stages after 30 and 240 min. The obtained results confirm that the one-step mechanochemical synthesis is a powerful technique for the preparation of nanocrystalline bismuth ferrite suitable for further ceramic processing.

Acknowledgments

This work was supported by Ministry of Education and Science of Republic of Serbia through projects III45007 (Zero- to Three-Dimensional Nanostructures for Application in Electronics and Renewable Energy Sources: Synthesis, Characterization and Processing) and COST MP0904 Action (SIMUFER).

References

- [1] W. Erenstein, N.D. Mathur, J.F. Scott, *Nature*, 442 (2006) 759-765.
- [2] M.I. Morozov, N.A.Lomanova, V.V.Gusarov, *Russian J. Gen. Chem.*, 73,11 (2003) 1676-1680.
- [3] S.T.Zhang, M.H.Lu, D.Wu, Y.F.Chen, N B.Ming, *Appl. Phys. Lett.*, 87 (2005) 262907.
- [4] M. Kumar, V.R.Palkar, K.Srinivas, S.V.Suryanarayana, *Appl. Phys. Lett.*, 76 (2000) 2764-2766.
- [5] Y.P. Wang, L. Zhou, M.F. Zhang, X.Y. Chen, J.-M. Liu, Z.G. Liu, *Appl. Phys. Lett.*, 84 (2005) 1731-1773.
- [6] G. Catalan, J.F.Scott, *Adv. Mat.* 21 (2009) 2463-2485.
- [7] G. Scholz, R. Stösser, J. Klein, G. Silly, J.Y. Buzaré, Y. Lagigant, B. Ziemer, *J.Phys.: Condens. Matter* 14 (2001) 2101-2117.
- [8] J. K. Kim, S.S. Kim, W.-J. Kim, *Mater. Lett.*, 59 (2005) 4006-4009.
- [9] J.-C. Chen, J.-M. Wua, *Appl. Phys. Lett.* 91 (2007)182903.
- [10] X. M. Lu, J.M. Xie, Y.Z. Song, J.M.Lin, *J. Mater. Sci.*, 42 (2007) 6824-6827.
- [11] S.Li, Y.-H. Lin, B.-P. Zhang, Y.Wang, C.-W. Nan, *J.Phys.Chem. C*, 114 (2010) 2903-2908.
- [12] Z.Dai, Y.Akishige, *J.Phys. D: Appl. Phys.* 43 (2010) 445403.
- [13] E.C.Aguiar, M.A.Ramirez, F.Moura, J.A.Varela, E.Longo, A.Z.Simoes, *Ceram. Int.* 31 (1) (2013)13-20.
- [14] I. Szafraniak, M. Polomska, B. Hilczer, A. Pietraszko, L. Kepinski, *J. Eur. Ceram. Soc.*, 27 (2007) 4399-4402.
- [15] C. Suryanarayana, *Prog. Mater. Sci.*, 46 (2001) 1-184.
- [16] A. Calka, D. Wexler, *Nature* 419 (2002) 147-151
- [17] R.K. Tiwary, S.P.Narayan, O.P.Pandey, *J. Min. Metall. B* 44 (2008) 91-100.
- [18] N. Burgio, A. Iasonna, M. Magini, S. Martelli, F. Padella, *Il Nuovo Cimento*, 13D (4) (1991) 459.
- [19] T. Rojac, M. Kosec, B. Malič, J. Holc, *J. Eur. Ceram. Soc.*, 36 (2006) 3711-3716.
- [20] A.A. Coelho, *Software Topas-Academic*, 2006.
- [21] C. Graves, S.K. Blower, *Mater. Res. Bull.*, 23 (1988) 1001-1008.
- [22] T. Atou, H. Faqir, M. Kikuchi, H. Chiba, Y. Syono, *Mater. Res. Bull.*, 33 (1998) 289-292.
- [23] E. Montanari, L. Righi, G.Calestani, A.Migliori, E. Gilioli, F. Bolzoni, F., *Chem. Mater.* 17 (2005) 1765-1773.